CHRONOS: A Cloud based Hybrid RF-Optical Network Over Synchronous Links

Maqsood Careem, Monette Khadr, Ahmed F. Hussien, Dola Saha, Hany Elgala and Aveek Dutta

Department of Electrical and Computer Engineering

University at Albany, SUNY

Albany, NY - 12222

Email: {mabdulcareem, mkhadr, ahussein, dsaha, helgala, adutta}@albany.edu

Abstract—This paper presents CHRONOS, a *Cloud based Hybrid RF-Optical Network Over Synchronous Links*. The primary goal of this project is to design, build and maintain a multi-node, heterogeneous, wideband, scalable, hybrid and synchronous Cloud Radio Access Network (Cloud RAN or C-RAN), specifically to support emerging applications requiring both THz-optical and conventional sub-6GHz technologies like Wi-Fi and cellular networks. The novelty of the testbed is in enhancing the core capabilities of C-RAN in multiple directions by integrating synchronous RF and Optical links that is not considered for contemporary C-RAN deployments. The long term goal of this project is to utilize the testbed to enable practical research in wireless and optical communication with emphasis on new hardware and software architecture for signal processing. In this paper, we present the design, implementation and initial results of CHRONOS, in an indoor setting, with a clear path to a scalable and real-time network. Our results show synchronous reception across multiple edge nodes while achieving an aggregate bandwidth of 108Mbps using 20MHz OFDM waveform in each RF and optical paths.

Fig. 1: High level architecture of CHRONOS.

I. INTRODUCTION

The exponential growth in wireless data traffic [1], along with increased density and scale of devices make the sub-6GHz spectrum incapable of catering to the stringent latency requirements in emerging applications, like Virtual Reality (VR), Augmented Reality (AR) and Ultra Reliable Low Latency Communications (URLLC). Higher frequencies provide the much required bandwidth with harsher channel conditions and hence less explored for communication purposes. As the research community continues its efforts in isolated frequency bands (*e.g.*, sub-6GHz, mmWave and THz), we believe that the challenge lies in integrated and seamless communication across multiple swaths of the radio spectrum, while each is complementary to the other. This necessitates rethinking and redesigning the network architecture, where concurrent links may exist in a wide variety of spectrum and switching between frequencies or antennas require minimal control overhead. Therefore, we propose CHRONOS: A *Cloud based Hybrid RF-Optical Network Over Synchronous Links* to virtualize the Radio Access Network (RAN), where the signal processing is separated from the underlying hardware. This significantly reduces the requirement for specialized hardware as software takes the center stage and virtualized Base Stations (BSs) or Access Points (APs) become the norm.
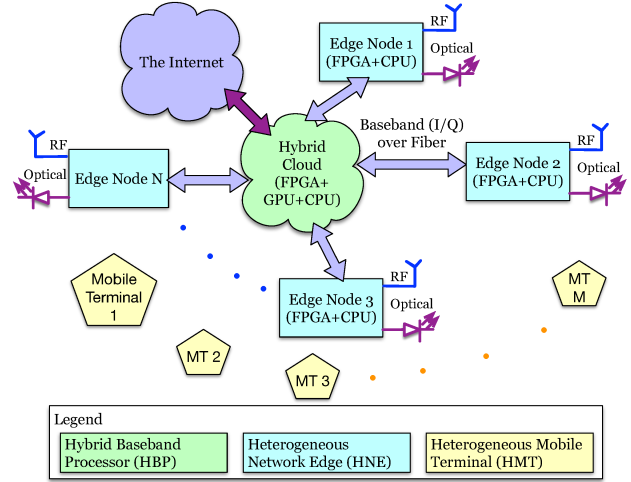
Figure 1 shows the architecture CHRONOS, which is an evolved version of the conventional *Cloud RAN* (C-RAN) [2]. It has *three* main components: 1) Hybrid Baseband Processor (HBP), 2) Heterogeneous Network Edge (HNE), and 3) Heterogeneous Mobile Terminal (HMT). The HBP is the hybrid cloud platform with multiple processing units, comprised of a combination of Field Programmable Gate Arrays (FPGAs), Graphics Processing Units (GPUs), and general purpose CPUs, specifically designed to simultaneously process *multiple* waveforms from *multiple* HNEs. The baseband (complex I/Q) signals are transported between the HNEs and the HBP over multimode fibers using efficient transport protocols and standardized packet formats. The HNE is the edge node or the wireless transceiver unit, which supports both sub-6GHz μ-wave, and optical THz bands to dynamically enable multiple wireless networks. It has multicore embedded processors and FPGAs to process time-critical signal processing (baseband may be one of such tasks). The HNEs are synchronized by a clock distribution network from the HBP. The HNE provides wireless connectivity to the HMT, equipped with similar wireless interfaces as the HNE. Often HMT will have less capabilities than HNE due to size and power constraints of mobile devices and include variety of devices, like evolved smart-phones, low power Internet-of-Things (IoT) devices, wearables etc. These terminals connect to the HBP through

HNE and eventually to the Internet.

The potential of C-RAN has been largely untapped. While the telecom industryis making some in-roads to early adoption, it is only limited to Distributed Antenna System (DAS) deployment for extending cellular coverage. We take a step forward to enhance this capability in our architecture. The unique features of our testbed are listed as follows:

1) **Heterogeneous (RF-Optical) Edge:** In addition to RF wireless access technologies, optical wireless access, specifically Visible Light Communications (VLC) or the Li-Fi technology offers high data rate using densely distributed light fixtures of existing illumination infrastructure [3]. It improves spectral efficiency over an area, enables data aggregation from multiple fixtures and relieves a large portion of RF resources. Since usage of mobile devices change over time, wireless access technologies of different coverage ranges and spectrum bands (sub-6GHz and optical THz bands) must coexist for improved performance for mobile devices under various applications.

2) **Hybrid Cloud based DSP:** Since Digital Signal Processing (DSP) (baseband or otherwise) is more malleable using a hybrid combination of general purpose processors, graphics processors and reconfigurable hardware, it enables detection and processing of different waveforms, *e.g.*, Wi-Fi and Long-Term Evolution (LTE), at the same time. The variety of processing capability in the cloud ensures that a scheduler can instantiate DSP modules within a processing unit based on latency, power, link performance or any other application specific criteria. Since the baseband signal is aggregated from multiple antennas, the architecture inherently allows for joint inspection and analysis of these aggregated signals to enable a variety of applications, such as collaborative physical layer (PHY) or network multiple-input multiple-output (MIMO), which were not possible with conventional fixed-function C-RANs.

3) **On-demand Edge Processing:** The baseband signal processing is modularized and can be performed efficiently by splitting between the HNEs and the HBP, enabling delay-sensitive communications and applications. Furthermore, we preserve connection states (*e.g.*, IP anchoring) while seamlessly switching between access networks entirely in the signal domain, eliminating latencies imposed by higher layer processing. This capability makes this testbed a practical architecture to embrace the potential for joint signal processing, while meeting strict application deadlines for 5G.

4) **Synchronous Edge:** The clock is distributed to the HNEs, such that the phases of the local oscillators are identical in all HNEs. This synchronous transmission and reception from multiple antennas enable several collaborative PHY applications, which benefits from fine grain control of the clock. Localization, coordinated transmission and reception, interference cancellation, network and distributed MIMO are few examples of research areas that can be greatly advanced by leveraging synchronous clocks.

Collectively, these capabilities are significant enhancements over conventional C-RAN , where the hardware and software components are optimized for a single wireless standard making those extremely brittle when exposed to emerging applications using a variety of waveforms.

II. Existing Testbeds

The importance of practical experiments and evaluation of mobile wireless networking research has lead to the development of multiple institutional and community testbeds, which *partially* overlap with our proposed system. Table I enlists the features of these testbeds where most operate in fixed frequency ranges, *e.g.*, sub-6GHz band, visible light spectrum, mmWave or higher frequency ranges. The future of wireless networks is not to sustain communication in isolated bands, but to integrate multiple spectrum with different channel characteristics such that they complement each other and seamless transitions are possible when necessary. This is the first initiative towards enabling simultaneous communication in sub-6GHz band as well as in the optical spectrum. To support on-demand access networks in different frequency bands, where the signal processing can be modularized and reused, a cloud-based reconfigurable radio architecture is the most practical design choice. ORBIT [4] and TurboRAN [5] claim to provide this, however none of them have heterogeneous frontends (RF and VLC), on-demand edge processing capabilities, hybrid (FPGA+GPU+CPU) cloud, dynamically reconfigurable signal processing and high-speed fiber fronthaul. In our testbed, the edge nodes are lightweight to create various scenarios, like labs with cubicles, staircases, corridors, etc. Often these testbeds do not allow for client mobility, which is a key feature of our proposed infrastructure. The LiRa [13] and LESA [14] are mainly focused on the integration of VLC as downlink transmission with Wi-Fi APs (only RF in uplink) at the MAC layer and the network layer, respectively.

III. CHRONOS Implementation

We implemented an indoor setup of CHRONOS with two HNEs, two HMTs and HBP as shown in Figure 2a. Each HNE and HMT is equipped with an USRP B210 [20], which is connected to an Intel NUC (NUC7i7BNH) with i7-7567U processor and 16GB DDR4 memory for faster processing of the I/O. Figure 2b shows one HNE and one HMT with RF and Optical frontends attached to it. Each B210 board has two transmit as well as two receive paths. We have used one RF and one optical link at both transmitter and receiver chains for simultaneous communication. B210 is designed to operate as MIMO transceiver, for which they share same local oscillator for the two transmit or receive paths. So, they are not tunable to separate frequencies, one for RF and one for the optical link. Hence, we choose 80MHz as our center frequency for both the paths. The baseband signal is up-converted to 80MHz center frequency from B210 and RF is transmitted as is using

TABLE I: Comparing `CHRONOS` with existing wireless testbeds

	C-RAN	sub-6GHz	Optical	mmWave & beyond
ORBIT [4]	✓	✓		
TurboRAN [5]	✓	✓		✓
WiSER [6], ROAR [7], WiNEST [8], ArgosNet [9], CORNET [10], Emulab [11]/PhantomNet [12]		✓		
LiRa [13], LESA [14]			✓	
WiMi [15], x60 [16], GigaNets [17], mmVital [18], TeraNova [19]				✓
CHRONOS	✓	✓	✓	work-in-progress
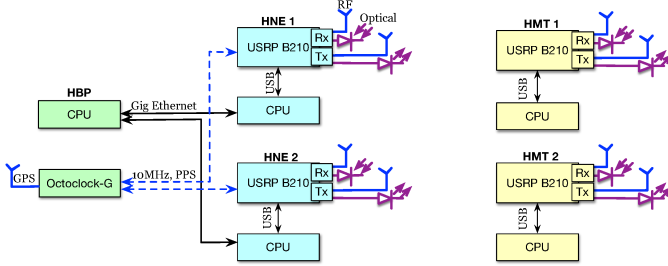
(a) Schematic diagram of current setup of the testbed.
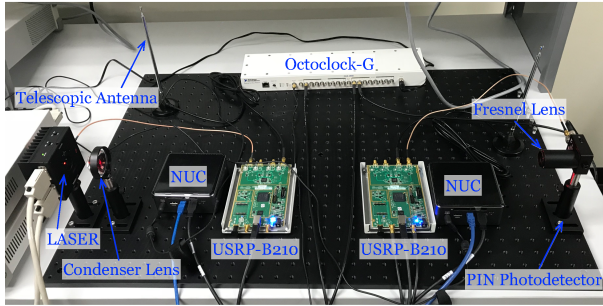
(b) One HMT and one HNE in the testbed.

Fig. 2: Testbed setup of `CHRONOS`

Fig. 3: Optical Frontends: transmitting LD to the left and capturing P-I-N PD to the right

a telescopic antenna. The optical frontend treats this signal as baseband and only utilizes the specified bandwidth (5MHz, 10MHz or 20MHz) around 80MHz frequency to convert to optical domain and transmit.

Most indoor optical wireless communication (OWC) systems rely on intensity modulation (IM) of the light source in baseband to realize inexpensive optical carrier modulation. This is mainly achieved through the elimination of mixers in conventional RF transmission chain [21]. At the demodulator, it is indeed difficult to achieve the required mixing efficiency of the coherent detector when the signal phase cannot be maintained and in non-directed propagation, *i.e.* non-line-of-sight (NLOS) scenarios [22]. Instead, direct detection (DD) is always deployed, where the photo-detector current is proportional to the received optical signal intensity, which for intensity modulation, is also the original modulating signal. Alternatively, in our setup, we reuse all building blocks of an RF transceiver including I-Q up-/down-converter and show the obtained bit-error performance results as a function of modulation order, bandwidth and signal-to-noise ration (SNR). We demonstrate that coherent transmission is still possible, and data must not always be encoded by means of IM/DD. It is
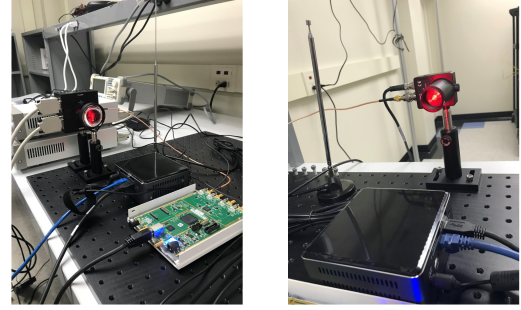
worth mentioning that toward reusing all building blocks of a conventional RF based OFDM transceivers, the polar-OFDM (P-OFDM) was proposed [23]. It uses real and imaginary parts of a complex-valued OFDM signal, thus also greatly improving the spectral efficiency of optical OFDM transmission.

The optical frontend is composed of the HL63163DG laser diode (LD) and the PDA10A P-I-N photodiode (PD) modules from Thorlabs. The LD is biased through the TCLDM9 mount to 70 mA and is attached to current and temperature controllers which protect the LD from damage. An aspheric collimating lens with 40mm focal length is controlling the LD field of view to ensure a parallel light rays beam, and thus obtain the required coverage based on the target distance. On the receiver side a fresnel lens with 25mm focal length is attached to the PD to collect the incident light onto the PD active area, and thus have high signal quality. One B210 feeds the LD mount with the transmitting signal, whereas on the receiver side another B210 captures the received signal for further processing. The optical frontend can be shown in Figure 3. The PD module captures the emitted optical signal, converts it into electrical and amplifies the electrical signal using a transimpedance-amplifier (TIA).

The USRPs are synchronized using Octoclock-G and the HNEs are connected over Gigabit Ethernet to move the signals between HNEs and HBP. Octoclock-G provides a 10MHz clock to the USRPs, as well as a Pulse-Per-Second (PPS) signal. Currently, the HBP is an i7 quad-core processor, but we are working towards integrating GPUs as well FPGAs into it to make it a hybrid cloud platform capable of meeting latency requirements of 5G and beyond. We will also update the Cat-6 Ethernet cables with Fiber Optic cables for faster fronthaul communication.

A. Baseband Processing

We have implemented both the transmitter and receiver baseband of IEEE 802.11a/g [24] in MATLAB and currently pre-processing as well as post-processing the signal to benchmark link capabilities. Currently we are generating our MAC frame and adding Frame Check Sequence (FCS) to create a PSDU. It is then modulated and encoded, followed by pilot insertion, IFFT and cyclic prefix addition. The baseband signal, thus generated, is stored in a binary file, which is forwarded to the USRP to be transmitted by both RF and Optical paths. We may choose to transmit same or different signal in the two paths.

At the receiver side, timing and synchronization block provides start of the packet, which is used in other modules. Long preamble is also extracted for channel estimation, which is used in data recovery phase. The SIGNAL Symbol is demodulated to receive the Modulation and Coding Scheme (MCS) as well as length of the packet. This information is used to demodulate rest of the packet after FFT and equalizer blocks. Once the data bits are recovered, we perform CRC check to determine if the packet was received correctly. We perform the receiver side signal processing on the captured binary data file after the experimentation.

B. Simultaneous Communication in RF and Optical

```
$ ./tx_samples_file_simultaneous --freq1 80e6
--freq2 80e6 --rate 5e6 --gain1 80 --gain2 60
--subdev="A:A A:B" --channel=0,1 --ant TX/RX
--ref=internal --repeat --spb 10000
--file1 /media/ramdisk/RF/RFTx.dat
--file2 /media/ramdisk/Opt/OptTx.dat

Creating usrp device with: serial=310733F...
-- Setting master clock rate selection:'automatic'
-- Setting clock rate 16.000000 MHz...
Using Device: Single USRP: Device:B-Series B210
Setting TX Rate: 5.000000 Msps...
-- Setting clock rate 40.000000 MHz...
Setting TX Freq of channel 0: 80.000000 MHz
Setting TX Freq of channel 1: 80.000000 MHz
Setting TX Gain of channel 0: 80.000000 dB
Setting TX Gain of channel 1: 60.000000 dB
Detecting which channels to use --successful
-- Setting clock rate 20.000000 MHz...
Buffer Size: 10000
Num of simultaneous transmissions : 2
```

Listing 1: Simultaneous transmission from single USRP.

We have implemented a C wrapper function for simultaneous transmission from multiple files, which accesses UHD APIs underneath to stream multiple signal streams to the USRP. A sample output of that code is shown in Listing 1 where each of the transmit chain is separately tunable to multiple parameters, like frequency, gain, files. Similarly, at the receiver end, another code is implemented to receive the two streams and store them in multiple files. We had to increase the buffer size to transmit/receive two simultaneous 20MHz links. We also used *ramdisk* to get the data faster from
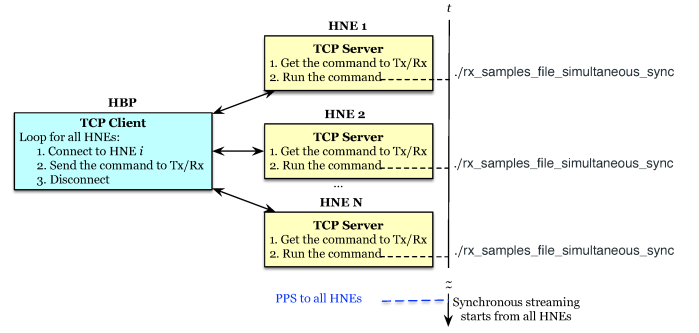

Fig. 4: Timing diagram for synchronous reception from multiple HNEs.

the memory and minimize the write time of the files in hard disk.

C. Synchronization

We have synchronized the internal clocks of the HNEs using the 10MHz external clock provided by the Octoclock-G, as shown in Figure 2a. However, streaming of data from all USRPs in all the HNEs should start at the same time to ensure that data processing can be done with synchronized set of received or transmitted data set. Hence, we have written a controller in the HBP to start the packet transmission or reception from each of the HNEs over a TCP connection. However, we use the PPS signal from the Octoclock-G to reset the clock of all the HNEs and they start transmitting or receiving after a known amount of time (*e.g.*, $2secs$) such that the streams start transmitting or receiving at the exact clock. Figure 4 shows the timing diagram of the synchronization as each HNE starts to execute the code at different times. However, the streaming from USRP starts only after all the HNEs receive a synchronous PPS signal. A sample output of that code is shown in Listing 2 where PPS is used to start the reception.

To verify the synchronization, we performed three tests and correlation plots are shown in figure 5. First, we transmitted RF from one HMT and received with two antennas in HNE, and correlate with known preamble. Figure 5a shows that there is no delay in the two signals indicating the two chains are synchronous. Secondly, we transmit RF signal from one HMT and receive it at two separate HNEs, which are synced using PPS signal. Figure 5b shows that there is no delay in the two signals. Finally, we also transmit both RF and Optical links from one HMT and receive from another HMT. Figure 5c shows there is no delay between the two paths. Although we believe that the Optical path will have a delay as it passes through Optical frontend, but it is less than one sample duration in 20MHz bandwidth, which is $50ns$.

IV. Benchmark Results

We were able to transmit and receive simultaneously over RF as well as Optical links, each spanning upto 20MHz bandwidth. We used IEEE 802.11a/g modulation and coding rate to reach up to 54Mbps physical layer data rate in one link.
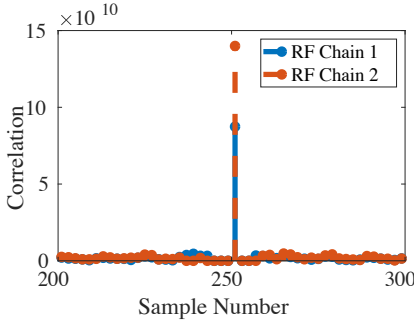
(a) Scenario 1 shows synchronous reception from two RF chains in the same board.
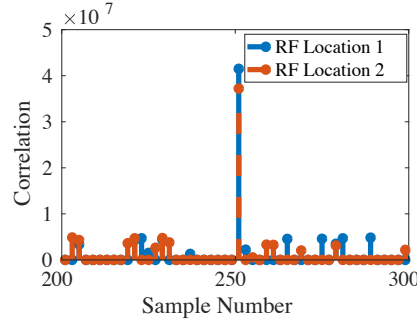
(b) Scenario 2 shows the synchronous reception from two different boards, synced using PPS signal.
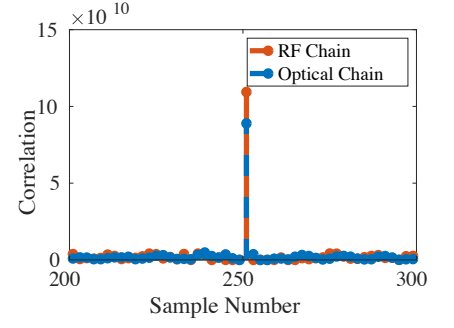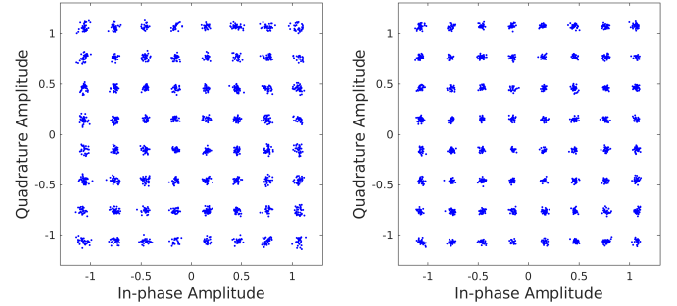
(c) Scenario 3 shows synchronous reception from an RF and and Optical path in the same board.

Fig. 5: Synchronization Output

```
$ ./rx_samples_file_simultaneous_sync --freq1 80e6
--freq2 80e6 --rate 20e6 --gain1 20 --gain2 20
--subdev="A:A A:B" --channel=0,1 --ref=external
--nsamp 1000000 --sync=pps --secs=2.5
--file1 /media/ramdisk/file_13.dat
--file2 /media/ramdisk/file_23.dat

Setting master clock rate selection: 'automatic'.
-- Setting clock rate 16.000000 MHz...
Setting RX Rate: 20.000000 Msps...
-- Setting clock rate 20.000000 MHz...
Setting device timestamp to 0...
--1) catch time transition at pps edge
--2) set times next pps (synchronously)
External 10 MHz clock locked++++++
Setting RX Freq of channel 0: 80.000000 MHz...
Setting RX Freq of channel 1: 80.000000 MHz
Setting RX Gain of channel 0: 20.000000 dB
Setting RX Gain of channel 1: 20.000000 dB
Begin streaming 1000000 samples, 2.500000
seconds in the future...
Done!
Buffer Size: 10000
Num of simultaneous transmissions : 2
```
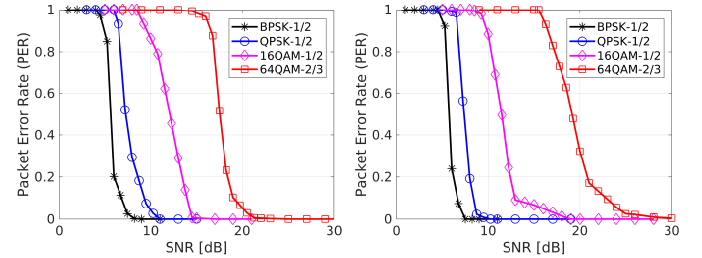
Listing 2: Synchronous reception from multiple USRPs.

Using simultaneous transmissions, we were able to achieve 108Mbps instantaneous PHY data rate.

Figure 6 portrays the constellation diagrams after equalization (as described in §III-A) for 64QAM modulated signals at 2/3 coding rate for the RF and Optical links respectively. We have chosen Minimum Mean Square Error (MMSE) for our equalization algorithm. The 64QAM modulated signals were demodulated correctly at 24dB.

We also measured the packet error rate for different MCS values in the RF and Optical links. The packet length remaining constant at 1000 bytes, we varied the transmit gain to change the SNR. Figure 7 shows the PER for BPSK, QPSK and 16QAM modulated signals at $1/2$ coding rate and 64QAM modulated signals at $2/3$ coding rate according to the wireless LAN non-HT format for OFDM modulation.

(a) Optical link.

(b) RF link.

Fig. 6: 64QAM constellation diagrams for Optical and RF links both at SNR = 24dB.

(a) Optical link.

(b) RF link.

Fig. 7: Packet Error Rate of Optical & RF links at 80MHz center frequency and 5MHz bandwidth.

V. LIMITATIONS AND CHALLENGES

The first and foremost limitation is caused by the chosen USRP board in the testbed. Although the B210 is capable of providing two simultaneous transmit/receive signal chains, these chains are controlled by a single local oscillator. Hence, in our case, both the RF and Optical chains are forced to transmit/receive over the same carrier frequency. Moreover, the B210s have a frequency coverage that starts from 70 MHz till 6 GHz. Even though these values are preferable for RF transmissions, as it covers FM and TV broadcast, cellular, GPS, WiFi, ISM, and more, however, these values push the boundaries of our Optical frontends. As a compromise, the

carrier frequency is set to 80 MHz, far below the expected operating frequency of the RF chain. On the other hand, the Optical chain had to suffer the loss of 70 MHz, and the full bandwidth of the optical chain is not utilized.

The second limitation is the delay between the RF and optical paths. In the RF chain, the antennas are directly connected to the USRPs, but the optical chain contains more components such as the laser source and the photodetector causing additional delays to the optical link. These delays might affect the synchronization of the packets simultaneously received via the RF and optical chains, when sampled at higher frequencies. This is to be noted that we did not notice any delay at $20MSamples/sec$ sampling rate. However, these delays are known and can be added to the signal path to ensure synchronous transmission over the air.

Conventionally, optical transmission is limited to non-coherent detection and uses the prevalent Intensity Modulation Direct Detection (IM/DD) technique. By definition, in intensity modulation, the transmitted waveform is modulated onto the instantaneous power of the optical carrier. On the receiver side, the photo-detector uses the down conversion technique and produces a photo-current proportional to the incoming signal power. In our experiments, since the same hardware equipment is used to receive both the RF and Optical signals, it is indispensable to consider coherent detection rather than the customary IM/DD technique. Clearly, the optical set up might have limited multipath reflections due to the bounded space and the LASER transmitting properties. Yet, the fact that coherent detection is viable in VLC gives a lot of insight for future work and further investigation.

Our current setup has general purpose processing units to move the data to and from USRPs, and is not capable of meeting real time stringent latency requirements of some of the wireless access protocols, like Wi-Fi and emerging applications, like Virtual Reality. Hence, most logical path for us is to a) update the USRP boards with FPGAs for faster processing at the HNE, b) change the Ethernet connection to optical for faster fronthaul and c) add FPGA and GPU blades in the Cloud for real time processing of the data and enable a true C-RAN architecture.

VI. CONCLUSION

In this paper, we explored the feature set and their performance of a next generation RF-optical C-RAN. The synchrony among the various components within the testbed opens new avenues of research in wireless networks that were not possible before. Through this exercise, we also realized concrete steps required to scale-up the testbed to support multiple HNE and HMT nodes. This can be accomplished by incorporating programmable logic (FPGA) in the HBP for real-time signal processing as well as high performance SDR (*e.g.*, USRP X310) at the HNE and HMTs to support simultaneous multi-band, RF-optical communication. A key challenge to scalability is the efficient resource allocation at the HBP and energy efficient fronthaul communication, which are the two key focus areas in the next iteration of CHRONOS.

REFERENCES

[1] "Cisco visual networking index: Global mobile data traffic forecast update, 2016 - 2021," *https://www.cisco.com/c/en/us/solutions/collateral/service-provider/visual-networking-index-vni/mobile-white-paper-c11-520862.html*, 2017. White Paper.

[2] A. Checko, H. L. Christiansen, Y. Yan, L. Scolari, G. Kardaras, M. S. Berger, and L. Dittmann, "Cloud ran for mobile networks a technology overview," *IEEE Communications Surveys Tutorials*, vol. 17, pp. 405–426, Firstquarter 2015.

[3] H. Elgala, R. Mesleh, and H. Haas, "Indoor optical wireless communication: potential and state-of-the-art," *Communications Magazine, IEEE*, vol. 49, no. 9, pp. 56–62, 2011.

[4] "ORBIT GEN 3 - Enhancing the ORBIT Testbed with LTE and Cloud Radio Processing. WINLAB, Rutgers University." https://www.nsf.gov/awardsearch/showAward?AWD_ID=1513110.

[5] "TurboRAN: Testbed for Ultra-Dense- Multi-Band Control and Data Plane Split Radio Access Networks of the Future." https://www.nsf.gov/awardsearch/showAward?AWD_ID=1730650.

[6] "WiSER Dynamic Spectrum Access Platform and Infrastructure. University of Colorado at Boulder." https://www.nsf.gov/awardsearch/showAward?AWD_ID=1305405.

[7] "ROAR - A Research Infrastructure for Real-time Opportunistic Spectrum Access in Cloud based Cognitive Radio Networks. Georgia Southern University." https://www.nsf.gov/awardsearch/showAward?AWD_ID=1405670.

[8] "WiNEST: A Prototype for a City-scale "Living Laboratory" for Wide-area Wireless Experimentation." https://www.nsf.gov/awardsearch/showAward?AWD_ID=1629833.

[9] "ArgosNet: A Reconfigurable Multi-Cell Research Platform for Massive Multiple Input Multiple Output (MIMO) Networks, William Marsh Rice University." https://www.nsf.gov/awardsearch/showAward?AWD_ID=1405937.

[10] "Radio Testbed Upgrade to Enable Wideband and MIMO Experiments." https://www.nsf.gov/awardsearch/showAward?AWD_ID=1629935.

[11] "EmuLab. University of Utah." https://www.emulab.net/.

[12] "PhantomNet: An End-to-End Mobile Network Testbed." https://www.nsf.gov/awardsearch/showAward?AWD_ID=1305384.

[13] S. Naribole, S. Chen, E. Heng, and E. Knightly, "Lira: A wlan architecture for visible light communication with a wi-fi uplink," in *2017 14th Annual IEEE International Conference on Sensing, Communication, and Networking (SECON)*, pp. 1–9, June 2017.

[14] "NSF Engineering Research Center for Smart Lighting. Rensselaer Polytechnic Institute, the University of New Mexico, and Boston University." https://www.nsf.gov/awardsearch/showAward?AWD_ID=0812056.

[15] "WiMi: A Reconfigurable Platform for Millimeter-Wave Wireless Networking and Sensing. University of Wisconsin-Madison." https://www.nsf.gov/awardsearch/showAward?AWD_ID=1506657.

[16] "X60: A Cross-Layer Reconfigurable Multi-Gigabit WLAN Testbed at 60 GHz, University at Buffalo." https://www.nsf.gov/awardsearch/showAward?AWD_ID=1629929.

[17] "GigaNets: A Path to Experimental Research in Millimeter Wave Networking." https://www.nsf.gov/awardsearch/showAward?AWD_ID=1518632.

[18] "60 GHz Millimeter-Wave Testbed for Multi-Gigabit Wireless Networking." https://www.nsf.gov/awardsearch/showAward?AWD_ID=1730083.

[19] "TeraNova: An Integrated Testbed for True Terahertz Communications." https://www.nsf.gov/awardsearch/showAward?AWD_ID=1730148.

[20] E. Research, "USRP B210." https://www.ettus.com/product/details/UB210-KIT.

[21] H. Elgala, R. Mesleh, and H. Haas, "Indoor optical wireless communication: potential and state-of-the-art," *IEEE Communications Magazine*, vol. 49, no. 9, 2011.

[22] J. M. Kahn and J. R. Barry, "Wireless infrared communications," *Proceedings of the IEEE*, vol. 85, no. 2, pp. 265–298, 1997.

[23] H. Elgala and T. D. Little, "Polar-based ofdm and sc-fde links toward energy-efficient gbps transmission under im-dd optical system constraints," *Journal of Optical Communications and Networking*, vol. 7, no. 2, pp. A277–A284, 2015.

[24] IEEE Computer Society : LAN/MAN Standards Committee, *Part 11: Wireless LAN Medium Access Control (MAC) and Physical Layer (PHY) Specifications*.